Poly(ADP-ribose) polymerase (PARP) is critically involved in liver ischemia/reperfusion-injury.

Short title: PARP is critically involved in liver I/R-injury

Sanae Haga, PhD,[a] Akira Kanno, PhD,[b] Naoki Morita, PhD,[c] Shigeki Jin, PhD,[d] Kotaro Matoba, MD,[d] Takeaki Ozawa, PhD,[e] and Michitaka Ozaki, MD, PhD [a,f]

[a] Department of Biological Response and Regulation, Faculty of Health Sciences, Hokkaido University, Sapporo, Japan

[b] Department of Environmental Applied Chemistry, Faculty of Engineering, University of Toyama, Toyama, Japan

[c] Bioproduction Research Institute, National Institute of Advanced Industrial Science and Technology (AIST), Sapporo, Japan

[d] Department of Forensic Medicine, Graduate School of Medicine, Hokkaido University, Sapporo, Japan

[e] Department of Chemistry, School of Science, The University of Tokyo, Tokyo, Japan

[f] Laboratory of Molecular and Functional Bio-Imaging, Faculty of Health Sciences, Hokkaido University, Sapporo, Japan

Author contributions. M. Ozaki and T. Ozawa designed research; M. Ozaki, S. Haga, A. Kanno and N. Morita performed research; S. Haga, S. Jin, K. Matoba and M. Ozaki analyzed data; and M. Ozaki wrote the paper.

Corresponding author.
Michitaka Ozaki M.D., Ph.D.
Department of Biological Response and Regulation
Faculty of Health Sciences, Hokkaido University
N12, W5, Kita-ku, Sapporo, Hokkaido, 060-0812 Japan
Tel.: +81-11-706-3337 /-3498
Fax: +81-11-706-3337 /-3498
E-mail address: ozaki-m@med.hokudai.ac.jp

ABSTRACT

Background: Poly(ADP-ribose) polymerase (PARP) is a DNA-repairing enzyme activated by extreme genomic stress, and therefore is potently activated in the remnant liver suffering from ischemia after surgical resection. However, the impact of PARP on post-ischemic liver injury has not been elucidated yet.

Materials and methods: We investigated the impact of PARP on murine hepatocyte/liver injury induced by hypoxia/ischemia, respectively.

Results: PJ34, a specific inhibitor of PARP, markedly protected against hypoxia/reoxygenation (H/R)-induced cell death, though z-VAD-fmk, a pan-caspase inhibitor similarly showed the protective effect. PJ34 did not affect H/R-induced caspase activity nor caspase-mediated cell death. z-VAD-fmk also did not affect the production of PAR (i.e., PARP activity). Therefore, PARP- and caspase-mediated cell death occurred in a mechanism independent of each other in H/R.

H/R immediately induced activation of PARP and cell death afterwards, both of which were suppressed by PJ34 or Trolox, an antioxidant. This suggests that H/R-induced cell death occurred redox-dependently through PARP activation. H/R and OS induced nuclear translocation of apoptosis inducing factor (AIF, a marker of parthanatos) and RIP1-RIP3 interaction (a marker of necroptosis), both of which were suppressed by PJ34. H/R

induced PARP-mediated parthanatos and necroptosis redox-dependently. In mouse experiments, PJ34 significantly reduced serum levels of AST, ALT & LDH and areas of hepatic necrosis after liver ischemia/reperfusion, similar to z-VAD-fmk or Trolox.

Conclusions: PARP, activated by ischemic damage and/or oxidative stress, may play a critical role in post-ischemic liver injury by inducing programmed necrosis (parthanatos and necroptosis). PARP inhibition may be one of the promising strategies against post-ischemic liver injury.

Keywords: ischemia/reperfusion; hypoxia/reoxygenation; oxidative stress; PARP; parthanatos; necroptosis

Introduction

Poly(ADP-ribose) polymerase (PARP), commonly known as a DNA-repairing enzyme, is activated by extreme genomic stress and breakage of DNA. It is involved in the repairing processes of cells with damaged DNA, thus protecting cells from death. PARP generates and adds poly[ADP-ribose] (PAR) to proteins (protein ADP-ribosylation, PARylation).[1–3] Catalytically generated PAR by PARP act primarily as scaffolds for the recruitment of DNA-repairing enzymes. It has been also known to be involved in various pathological events including cell death and inflammation. PARP is suggested to promote programmed/non-programmed cell deaths such as necrosis, parthanatos and necroptosis in various cells. Excessively activated PARP directly induces necrosis by consuming/depleting NAD(+) and ATP.[4] Additionally, PARP is suggested to be associated with the other types of programmed necrosis such as parthanatos and necroptosis. Parthanatos, a necrotic type of programmed cell death, is caused by DNA damage, excessive activation of PARP, production of PAR, and the following nuclear translocation of apoptosis-inducing factor (AIF) from mitochondria.[5] The interaction of PARP and receptor-interacting protein (RIP) has also been reported, suggesting induction of necroptosis, another type of programmed necrosis, by PARP-activation.[6–8] However, the interrelationships of these cell deaths (necrosis, parthanatos and necroptosis) and the

impact on various pathological situations including ischemia/reperfusion (I/R) still remains unclear.

I/R of liver is an unavoidable event in liver surgery, transplantation and cancer embolization-therapies, which sometimes cause serious liver failure leading to life-threatening complications. To date, many studies have been performed in order to prevent I/R-induced liver injury.[9–16] The mechanism of I/R-induced liver injury, however, appears complicated such that we have not yet succeeded in the development of a clinically effective therapy.[17] During liver ischemia, necrosis induced by a lack of ATP, mainly accounts for ischemic liver injury. Reactive oxygen species (ROS) generated immediately after I/R have been shown to trigger and enhance post-ischemic liver injury.[18–22] ROS generated in hepatocytes lead to the redox-dependent activation of caspases (i.e. apoptosis) that contributes directly to liver injury, and the NFκB-dependent production of proinflammatory cytokines that contributes indirectly to sterile inflammation and the enhancement of injury.[22]

Regarding the ROS-induced programmed cell death that emerges after I/R and hypoxia/reoxygenation (H/R), extensive studies have been performed, mainly focusing on apoptotic cell death thus far.[10,11,18,22–25] Apoptosis is a non-lytic (non-necrotic) type of programmed cell death that occurs in caspase- and redox-dependent manners.[26–28]

Caspases are a group of cysteine proteases that make up cascade signaling pathways and cause cells to undergo cell death (apoptosis).[29] Interestingly, certain caspases are involved in regulating immune system through the activation of cytokines (e.g. IL-1β).[30,31] Because caspases cleave enzymes with a cysteine residue, they may also inactivate other molecules having a cysteine in their active site, including PARP.[32] Therefore, caspases and PARP may affect/interact with each other in induction process of programmed cell death. Caspases have widely attracted attention as potent therapeutic targets against various diseases and pathological situations, including H/R and I/R of cells and organs, respectively.[18,22,30,31,33] However, inhibition of caspases only partially improves I/R-induced liver injury.[18,24,34–36] These facts suggest that not only caspases but also other molecules including PARP may play important roles in I/R-induced injury.

In the present study, we examined the involvement of PARP in post-hypoxic/-ischemic injury of hepatocytes/liver, respectively. We showed the impact of PARP inhibition on suppression of H/R- or I/R-induced injury of hepatocytes/liver, and proved that H/R induces redox-dependently PARP-mediated programmed cell death, parthanatos and necroptosis, rather than caspase-mediated apoptosis.

Materials and methods

Cell culture and reagents

AML12 cells, established from hepatocytes from a mouse transgenic for human transforming growth factor-α (TGF-α), express high levels of human TGF-α and lower levels of mouse TGF-α (ATCC, Manassas, VA, USA). Cells were maintained at 37°C and 5.0% CO_2 in Dulbecco's modified Eagle's (DMEM) /Nutrient Mixture F-12 (Nacalai Tesque, Kyoto, Japan) supplemented with 10% fetal bovine serum (FBS) and 1× ITS-A (Thermo Fisher Scientific). PJ34 (a specific PARP inhibitor, Merck, Darmstadt, Germany), staurosporine (STS, Merck), Jo2 (a Fas-ligand; BD Biosciences, Franklin Lakes, NJ, USA), z-VAD-fmk (a pan-caspase inhibitor; R&D Systems, Minneapolis, MN, USA) and Trolox (antioxidant; Merck) were administered to AML12 mouse liver cells. All other chemicals were of analytical grade and used without further purification.

Protein expression in cells and liver tissue

Whole-cell protein extracts (5 μg) were prepared for western blot analysis according to a standard analysis protocol. Briefly, whole-cell protein extracts were separated by 10% sodium dodecyl sulfate-polyacrylamide electrophoresis and transferred to polyvinylidene fluoride (PVDF) membranes. Western blot analysis of PVDF membranes was performed with appropriate antibodies: caspase 8 (1:200; sc-7890; Santa Cruz, Dallas, TX, USA), pro-caspase 3 (1:1000; #9665; Cell Signaling Technology [CST], Danvers, MA, USA), cleaved caspase 3 (1:1000; #9664; CST), PARP (1:1000; #9542; CST), PAR (2.5 μg/mL; ALT-804-220; Enzo Biochem Inc., Farmingdale, NY, USA), AIF (1:1000; #5318; CST), and β-actin (1:2000; #4970; CST). Because activated PARP ADP-ribosylated proteins, "PARP activity" was evaluated by the signal intensity of the production of PAR. For the expression analysis of proteins in some experiments, protein separation and detection were performed using an automated capillary electrophoresis system, Wes™

(ProteinSimple, San Jose, CA, USA), according to the manufacturer's protocol. Signals were detected with a horseradish peroxidase-conjugated secondary antibody, and visualized using Compass for SW software (ProteinSimple).

Hypoxia/Reoxygenation

Cellular hypoxic conditions were created and maintained in a modular incubator chamber (Billups-Rothenberg, San Diego, CA, USA) by flushing with a 95% N_2/5% CO_2 gas mixture for 10 min and then sealing the chamber. This method has been shown to achieve a pO_2 of 10 ± 5 Torr. [18,19,21,33] Following 5 h of hypoxia, AML12 cells were reoxygenated by opening the chamber and replacing the hypoxic medium (no-glucose DMEM [Thermo Fisher Scientific] without FBS) with oxygenated medium (high-glucose DMEM medium [glucose; 450 mg/dL; Sigma–Aldrich, St. Louis, MO, USA] supplemented with 10% FBS).

Monitoring and evaluation of cell survival and cell death

Cells at 40 - 50% confluence were seeded in a plate. Cell survival was determined by plating the cells in an xCELLigence System (Roche, Basel, Switzerland), which allows for automated non-invasive, real-time, and label free monitoring of live cells in culture. For the evaluation of cell death, we examined LDH release from hepatocytes into culture media. An LDH cytotoxicity detection kit (Takara Bio, Otsu, Japan) was used to measure LDH in culture media, according to the manufacturer's instructions. Briefly, LDH reaction mixture was added to each aliquot of medium taken from cell cultures. The absorbance at 490 nm was measured using a multi-well plate reader.

Translocation of AIF to nucleus in AML12 cells

The translocation of AIF from the cytosol to nucleus was immunocytochemically

observed by fluorescence microscopy. Cells were washed, fixed with 4% paraformaldehyde, and permeabilized with 0.2% Triton X-100 in PBS. Anti-AIF (CST) (1:100, 4ºC, overnight) and Alexa 488 (green) donkey anti-rabbit (Thermo Fisher Scientific) (1:300, room temperature, 2 h) were used as primary and secondary antibodies, respectively, for the immunofluorescent detection of AIF. Hoechst 33342 (blue) was used for specifically staining the nuclei of cells. The nuclear translocation of AIF by STS, Fas ligand (FasL), H_2O_2 or H/R with/without reagents (PJ34 or Trolox) was observed fluoroscopically. To quantify AIF-nuclear translocation, fluorescence intensity was measured 3 times for each of 20 cells and analyzed with ImageJ software (version 1.52a; National Institutes of Health, Bethesda, MD, USA). The AIF signals (green) of the nucleus (blue) were calculated by subtracting the AIF signals of the cytoplasm from the total AIF signals. The AIF signals of the nuclear region were defined as AIF-nuclear translocation.

Measurement of RIP1-RIP3 interaction by the optic probe in AML12 mouse liver cells

The structures of constructed cDNAs encoded fusion proteins used for measuring the interaction of mouse RIP1 and RIP3 on the basis of protein-fragment complementation (split luciferase reconstitution). [19] Hepatocytes infected with cDNA expressed chimeric proteins: mouse RIP3 fused to the N-terminal fragments of click beetle luciferase (CBR; CBR [1 - 413]; CBRN); and mouse RIP1 linked with the C-terminal fragment of CBR (CBR [395 - 542]; CBRC). When fusion proteins mutually interacted, CBRN and CBRC refolded correctly, and their bioluminescence activity was recovered. The RIP1-RIP3 interaction, namely, the reconstitution of split luciferase (CBRN and CBRC), was

monitored by measuring the recovered bioluminescence intensity of live cells with a luminometer (Kronos Dio, Atto Corp., Tokyo, Japan).

Animal experiments

Mice (C57BL6/J, male, 12 weeks of age) were fasted overnight before experiments. General anesthesia was induced by inhalation of the anesthetic, methoxyflurane (Metofane); heparin sulfate (100 U/kg body weight [BW]) was injected intravenously after laparotomy before liver ischemia. All vessels (hepatic artery, portal vein, and bile duct) to the left and median liver lobes were clamped, according to a previously described method.[37,38] After 60 min of liver ischemia, these vessels were unclamped, and circulation restored. Sham-operated control mice were subjected to laparotomy and closure without liver ischemia with/without administration of PJ34, z-VAD-fmk or Trolox. PJ34 (5 mg/kg BW), z-VAD-fmk (5 mg/kg BW) or Trolox (50 mg/kg BW) was administered intraperitoneally twice to mice 5 min before and 1 min after liver ischemia. Mice were sacrificed for the collection of liver and blood specimens 24 h after sham-operation and reperfusion (Fig. 6A). All animals were handled according to the uniform policies set forth by the Animal Care and Use Committee of Hokkaido University, which approved the present experiment (#16-0135).

Evaluation of post-ischemic liver injury

Liver specimens were excised and fixed in 10% buffered formalin, embedded in paraffin, and stained with hematoxylin and eosin (H & E). Biochemical analyses of serum aspartate aminotransferase (AST), alanine aminotransferase (ALT), and lactate dehydrogenase (LDH) were performed as indices of liver injury before and 24 h after hepatic ischemia.

Statistical analysis

Shapiro-Wilk's test was used to confirm normality of the data. Normally distributed data were analyzed by a Tukey-Kramer test to perform intergroup comparisons and expressed as mean ± standard deviation (S.D.). Non-normally distributed data were analyzed by a Kruskal-Wallis test with a Dann-Bonferroni post hoc test for multiple comparisons (a non-parametric test) and expressed as median and interquartile range. A value of $p < 0.05$ was considered significant. Statistical analysis was performed using SPSS, version 26, for all analyses (IBM, Armonk, NY).

Results

PARP is critical in hypoxia/reoxygenation-induced cell death of mouse liver cells

We first examined whether or not PARP-mediated cell death plays an important role in H/R-induced cell death, in addition to caspase-mediated cell death (apoptosis), because apoptotic cell death has been shown to be induced after I/R (or H/R), and considered to play a central role in post-ischemic injury (or post-hypoxic cell death).[10,11,18,19,21,23,24,39]

Five hours of hypoxia induced significant cell death after reoxygenation in AML12 mouse liver cells (**Fig. 1A, left panel**). H/R-induced cell death became marked within 12 h, and thereafter increased gradually until 36 h after H/R. We used PJ34, a specific PARP inhibitor, and z-VAD-fmk, a pan-caspase inhibitor, against H/R-induced

cell death to understand the role of PARP and caspases in the induction of cell death. Though both of these reagents significantly suppressed H/R-induced cell death, PJ34 was more effective in the suppression of cell death (more than 50% suppression) compared with z-VAD-fmk in the concentrations examined (about 20% suppression) (**Fig. 1A, right panel**). Importantly, PJ34 robustly suppressed an immediate cell death (LDH release), which continued more than 24 h after H/R.

We analyzed the signals associated with caspases (i.e., apoptosis) and PARP after H/R (**Fig. 1B**). H/R strongly activated caspase 3 peaked at 8 h after H/R, which may have eventually cleaved (inactivated) PARP. PARP (full length) was gradually decreased in its expression after H/R, and, accordingly, increased the cleaved form of PARP. The production of PAR observed after H/R was increased until 8 h, and thereafter suddenly decreased in accordance with caspase 3 activation. Because activated caspases cleave/inactivate PARP,[32] PARP was possibly cleaved/inactivated by the H/R-activated caspases. H/R induced caspase 3 activation, which was suppressed by z-VAD-fmk (**Fig. 1C**). PJ34, however, did not affect caspase activation at all, suggesting that PARP does not affect caspase-mediated signals activated by H/R.

The inhibition of PARP protected hepatocytes independently of caspases

In order to study more clearly and directly the effect of PARP on caspase-

mediated apoptotic cell death, we used STS and FasL to directly activate caspases and induce apoptosis in AML12 mouse liver cells (**Fig. 2**). Robust cell death by treatment with STS was observed even 4 h after treatment. The inhibition of PARP by PJ34 did not affect STS-induced liver cell death (**Fig. 2A, left panel**). Western blot analysis revealed that treatment with STS began to cleave/activate caspase 3 4 h after treatment, which peaked at 16 h after treatment and continued for at least 24 h (**Fig. 2A, right panel**). Full length of PARP and the production of PAR were not increased after the treatment, but rather reduced gradually in accordance with the activation of caspase 3. PJ34 did not affect caspase-mediated cell death in STS-treated cells.

Treatment with Jo2 (4 μg/ml), a FasL, slowly induced cell death (16 - 24 h after the treatment). Also, in this case, PARP inhibition by PJ34 did not affect Jo2-induced liver cell death (**Fig. 2B, left panel**). Treatment with Jo2 cleaved caspase 3 and eventually PARP, especially 16 - 24 h after the treatment, and reduced the production of PAR (**Fig. 2B, right panel**). PJ34 was not associated with FasL-induced, caspase-mediated cell death. These data indicate that STS- or Jo2-induced, caspase-mediated cell death (i.e., apoptosis) occurred under a mechanism independent of PARP in AML12 mouse liver cells.

H/R-induced PARP activation (the production of PAR) depends on oxidative

stress, independent of caspases

Next, we examined whether or not the production of PAR by H/R-activated PARP is dependent on oxidative stress (OS) in AML12 mouse liver cells (**Fig. 3**). Though a small production of PAR was observed even before hypoxia, it started to increase immediately after reoxygenation and continued to increase for at least 8 h (**Fig. 3A, left blot**). The production of PAR was significantly reduced by pre-treatment with PJ34, but not with z-VAD-fmk (**Fig. 3A, middle & right blots**). The expression of PARP was kept at high levels despite 5 h-hypoxia (Reoxygenation 0 h), though β-actin was obviously decreased (**Fig. 3A, left**). PARP was partially cleaved 8 h after H/R, possibly by H/R-activated caspases. Pre-treatment with PJ34 suppressed the H/R-induced production of PAR very effectively without affecting PARP cleavage (**Fig. 3A, middle**). In contrast, z-VAD-fmk did not affect the production of PAR very much, even though it clearly inhibited the caspase-dependent PARP cleavage (**Fig. 3A, right**).

Because OS plays a critical role in the induction of post-ischemic/-hypoxic liver injury/cell death, we examined whether or not Trolox, an analog of vitamin E possessing antioxidant property, suppresses H/R-induced production of PAR in comparison with caspase activation (**Fig. 3B, C**). Pre-treatment with Trolox slightly but significantly suppressed the production of PAR and PARP, and its cleavage (**Fig. 3B**). Though H/R

induced activation of caspase 3 after H/R (**Fig. 3C**), Trolox did not suppress H/R-induced caspase activation. These data indicate that H/R-induced OS contributes to the production of PAR (i.e., PARP activation), rather than caspases.

Taken together, H/R activated PARP and produced PAR in a redox-dependent manner, independently of caspases.

Oxidative stress directly and immediately induced PARP activation (the production of PAR) and cell death

We investigated whether or not OS itself induces cell death through activation of the PARP-PAR pathway in AML12 mouse liver cells.

After treatment with H_2O_2 (1 mM), the cleavage of caspase 3/8 occurred 8 h or at later timepoints after treatment (**Fig. 4A**). In accordance with caspase activation, PARP was cleaved (inactivated) 8 to 16 h after treatment, which resulted in a transient reduction of the production of PAR. These data suggest that H_2O_2 directly and immediately induced PARP activation, which continued for at least 24 h. In contrast, caspases activated by H_2O_2 may have cleaved/inactivated PARP and transiently reduced the production of PAR.

Next, we examined the protective effect of PJ34 against H_2O_2-induced cell death using AML12 mouse liver cells. After treatment with H_2O_2, hepatocytes began to die immediately (1 - 2 h) and continued to die for 16 h (**Fig. 4B**). PJ34 apparently had a

protective effect against H_2O_2-induced cell death at all timepoints. It is noticeable that the induction of cell death by H_2O_2 was obvious even 2 h after the treatment, when caspases were not activated at all (**Fig. 4A**). This indicates that H_2O_2-induced immediate cell death was not mediated by caspases. The production of PAR was detected markedly after treatment with H_2O_2, though it was slightly recognized even before the treatment (**Fig. 4C**). The production of PAR was clearly inhibited by pre-treatment with PJ34.

These data indicate that OS may immediately induce and promote cell death in a PARP-dependent pathway.

H/R-initiated, OS-mediated activation of PARP leads to parthanatos and necroptosis

Because PARP did not affect caspase activation nor induce apoptotic cell death, we next studied whether or not OS or H/R induces other types of cell death through PARP activation. Parthanatos and necroptosis induce lytic (necrotic) type of cell death, and are considered to be related to PARP.[6,8,40] Furthermore, these cell deaths can potently cause sterile inflammation and propagate post-ischemic liver injury, than apoptosis.

The nuclear translocation of cytosolic AIF was immunocytochemically studied to detect parthanatotic cell death. Without stimulus, AIF was not observed in nuclei in AML12 mouse liver cells (**Fig. 5A**). Neither STS nor Jo2 induced the apparent nuclear

translocation of AIF, and, therefore, caspase-mediated machinery may not induce parthanatos. Treatment with H_2O_2 (1 mM) induced the nuclear translocation of AIF, which was suppressed by pre-treatment with PJ34. H/R induced the translocation of AIF into the nucleus in AML12 mouse liver cells (**Fig. 5B**), which was effectively inhibited by PJ34. The nuclear translocation of AIF by H/R was also inhibited by Trolox, an antioxidant. These data indicate that parthanatos is induced as an H/R-OS-PARP-mediated mechanism, suggesting the involvement of parthanatos in I/R-induced liver injury.

Next, we studied whether or not necroptosis is induced by OS or H/R through PARP activation. We previously reported that necroptosis is induced by OS or H/R in AML12 mouse liver cells.[19] Because the interaction of RIP1 and RIP3 molecules is required for the induction of necroptosis, we applied the optic probe to measure the interaction of these molecules in AML12 mouse liver cells.[19] H_2O_2 gradually induced RIP1-RIP3 interaction for more than 48 h in AML12 mouse liver cells, which was suppressed significantly by pre-treatment with PJ34 (**Fig. 5C**). This clearly indicates that OS-induced necroptosis is mediated by activated PARP. H/R induced RIP1-RIP3 interaction, which was also suppressed by PARP inhibition (PJ34; **Fig. 5D**) or antioxidant (Trolox; **Fig. 5E**). RIP1 and RIP3 began to interact gradually after H/R and achieved peak levels within 24 h after reoxygenation, which continued for at least 36 h. Trolox inhibited

RIP1-RIP3 interaction immediately and was effective enough until 36 h after H/R. These observations suggest that OS and PARP mediate H/R-induced RIP1-RIP3 interaction (i.e., necroptosis). Because the inhibition of PARP promoted to dissociate RIP1-RIP3 interaction at later timepoints after H/R (**Fig. 5D**), PARP may be involved in injury which emerges at later phase after I/R.

PJ34 inhibited AIF translocation and RIP1-RIP3 interaction induced by H/R or H_2O_2. This indicates that parthanatos and necroptosis were both downstream events of OS- or H/R-activated PARP. Hence, H/R may induce parthanatos and necroptosis through redox-dependently activated PARP, independently of caspases.

Inhibition of PARP markedly reduced post-ischemic liver injury in mice

Lastly, we examined how effectively PARP inhibition reduces I/R-induced liver injury in comparison with z-VAD-fmk or Trolox, using mouse model (**Fig. 6A**).

Administration of PJ34, z-VAD-fmk or Trolox alone showed no significant effects on blood biochemistry (ALT, AST and LDH) in sham-operated mice with no liver ischemia (**Fig. 6B**). Sixty minutes of liver ischemia induced severe liver injury 24 h after reperfusion in mice. Serum levels of ALT, AST and LDH were markedly increased 24 h after liver I/R. The increase of these enzyme levels was significantly and sufficiently suppressed by treatment with PJ34, as well as z-VAD-fmk or Trolox (**Fig. 6B**). In support

of this, histological examination of the post-ischemic liver tissue demonstrated existence of massive necrosis of the post-ischemic liver tissue. Liver injury was markedly improved by pre-treatment especially with PJ34 (**Fig. 6C**), though z-VAD-fmk or Trolox similarly reduced the necrotic areas of the post-ischemic liver tissue.

In liver tissue, full length and cleaved forms of PARP were detected in trace amounts even without ischemia (**Fig. 6D, left panel**). The expression of PARP was obviously increased immediately after I/R, which was suppressed effectively by treatment with PJ34. The production of PAR was markedly increased along with increase of PARP by hepatic I/R, which was also reduced significantly by treatment with PJ34 (**Fig. 6D, right panel**). This indicates that PARP was certainly activated by hepatic I/R, which was effectively suppressed by PJ34.

In the *in vivo* experiment using mouse, PJ34 dramatically prevented liver from I/R-induced injury by suppressing PARP activation.

Discussion

To date, various types of cell death have been identified to occur as the result of signal-regulated and redox-dependent events in liver/hepatocytes.[18–20,34,41–43] Apoptotic cell death is best known in various hepatic pathological conditions, including acute and

chronic hepatitis, and post-ischemic liver. [20,22,25,34,35,44–47] Apoptosis commonly occurs in a caspase-dependent manner,[45] and has been considered to play a central role redox-dependently in I/R-induced liver injury (or H/R-induced cell death).[18,20,21] The present study, however, indicated that PARP may be similarly crucial and redox-dependent in H/R-induced cell death, and induced unique types of programmed cell deaths (parthanatos and necroptosis), but not apoptosis (**Fig. 1A**, **3B, C**).

Caspases potently activate PARP by inducing DNA fragmentation (apoptosis), but also inactivate PARP by directly cleaving it. So, there is some possibility that caspases are affecting PARP-mediated cell death. In the present study, H/R caused the immediate production of PAR (i.e., PARP activation), which gradually and robustly increased until the activated caspases cleaved PARP (**Fig. 1B**). The cleavage of PARP by H/R-activated caspases may have resulted in transient reduction of the production of PAR.

Inhibition of caspases by z-VAD-fmk did not affect H/R-induced production of PAR (**Fig. 3A**). On the contrary, inhibition of PARP did not affect STS-/FasL-induced cell death (**Fig. 2A, B**), nor H/R-induced caspase activation (**Fig. 1C**). Taken together, PARP- and caspase-mediated cell death machineries seem to function independently of each other, with the former appearing more redox-dependent (**Fig. 3B, C**).

Several lines of evidence suggest that this pathway potently plays an important

role in I/R-induced injury of brain, heart, intestines, lung, liver and limbs.[8,23,48–52] They showed the protective effect of some chemical PARP inhibitors against I/R-induced injury and inflammation of various organs/tissues in rodent models. However, the molecular mechanisms how excessively activated PARP induces cell death and what kind of programmed cell deaths are induced, have not been fully elucidated. Here in this study, we tried to clarify the molecular mechanism how PARP is involved in H/R-induced cell death or I/R-induced liver injury, in comparison with caspase activation (apoptosis) and OS. We showed that parthanatos and necroptosis, but not apoptosis, are certainly involved PARP-mediated cell death, and may be more redox-dependent than caspase-mediated cell death (apoptosis) (**Fig. 3B, C**).

Parthanatos is a kind of lytic type of programmed cell death that contributes to tissue/organ injury and potently enhances injury by inducing sterile inflammation in various pathological conditions.[4,8,23,53] The intrinsic cell death pathway mediated by PARP-PAR-AIF and its pathological roles have recently been described.[53,54] In the present study, OS induced the translocation of AIF into the nucleus, which was suppressed by PARP inhibition in AML12 mouse hepatocytes (**Fig. 5A, B**), suggesting the involvement of parthanatos in OS-triggered, PARP-mediated hepatocyte cell death. In contrast, STS/FasL did not induce AIF translocation, indicating that caspases do not contribute to

AIF-mediated parthanatotic cell death of hepatocytes. Necroptosis is another lytic type of programmed cell death. The interaction of RIP1 and RIP3 molecules is essential for the induction of necroptosis.[5,6,19,55,56] In the present study, OS and H/R persistently induced RIP1-RIP3 interaction, which were suppressed significantly by a PARP inhibitor (PJ34) or an antioxidant (Trolox) (**Fig. 5C, D, E**). This indicates that the induction of necroptosis by H/R is both redox- and PARP-dependent. Because an antioxidant suppressed H/R-induced PARP activation (the production of PAR) (**Fig. 3B**), H/R-triggered OS may send signals to induce RIP1-RIP3 interaction through PARP activation. It is notable that PARP inhibition reduced H/R-induced RIP1-RIP3 interaction markedly late after H/R (i.e., after the completion of the interaction). PARP inhibition may contribute to dissociation of RIP1 and RIP3 interaction in H/R (**Fig. 5D**). Though some reports suggest that the OS-RIP1/RIP3-PARP pathway mediates cell death,[6,7] our data, rather, suggest OS-activated PARP may play a role in sustaining the RIP1-RIP3 interaction and necroptosis in H/R-induced cell death (OS-PARP-RIP1/RIP3 pathway). PARP activated by OS may initiate and sustain liver injury by inducing parthanatos and necroptosis, respectively.

In mouse experiments, PARP inhibition (PJ34) undoubtedly suppressed I/R-induced liver injury of mouse (**Fig. 6B, C**). The inhibitors of caspases (z-VAD-fmk) or OS (Trolox) were also challenged against the post-ischemic liver injury, showing the

similarly significant effect against liver I/R injury (**Fig. 6B**). PARP- and caspase-mediated cell death occurred in a mechanism independent of each other in the present study. Therefore, PARP inhibition seems to be a highly potent therapeutic strategy against liver I/R injury, especially in combination with a caspase inhibitor.

In the present study, anti-inflammatory effect by PARP inhibition was not clear, though several reports have suggested that PARP is associated with inflammation in various organs, including the liver.[4,57–59] Activated PARP is known to promote inflammatory responses by activating the pro-inflammatory NF-κB.[4] Bacterial products (LPS) and inflammatory cytokines (interleukin [IL]-1, tumor necrosis factor [TNF]-α) also activate PARP and NF-κB. Interestingly, PARP, activated by reactive oxygen species (ROS), may be deeply involved in OS-induced inflammation. Inflammation enhances ROS generation in the tissue which will provoke and enhance tissue damage and inflammation. Because inflammation eventually induces an accumulation of damaged DNA, it will further activate PARP, DNA-repairing mechanisms, and inflammation.[4,60] PARP may be a key player for interconnecting ROS, DNA damage and inflammation in various pathological conditions. In fact, PARP has been shown to be associated with several pathological processes, including intestinal I/R-induced injury, stroke, myocardial infarction, and neurodegenerative disorders.[61–63] PARP, therefore, may play a major role

in liver injury and inflammation after I/R. Further study is required to understand the proinflammatory roles of PARP in parenchymal and non-parenchymal cells including hepatocytes and Kupffer cells, in regard to I/R-induced liver injury.

I/R (H/R)-activated caspases can cause apoptotic cell death with DNA fragmentation. However, the activated caspases seemed to cleave/inactivate PARP to achieve caspase-mediated cell death (apoptosis), though DNA fragmentation by activated caspases may initially activate PARP (**Fig. 7**). DNA damage caused by H/R- or I/R-induced OS will directly induce necrosis or activate PARP. The activated PARP may cause signal-regulated programmed cell death, such as parthanatos and necroptosis, via nuclear translocation of AIF and RIP1-RIP3 interaction, respectively. Parthanatos and necroptosis are crucially involved in I/R-induced liver injury, similar to apoptosis. These lytic types of cell death may provoke sterile inflammation and enhance injury in the post-ischemic liver.

There are some limitations to note in the present study. We only used male mice for the study of liver I/R experiment, eventually arising the potential question regarding the effectiveness of PARP inhibition in protection against liver I/R injury in female mice. There exist some reports stating the sex-differences of the intensity and mechanism of liver I/R injury in mice, showing that female mice are possibly more resistant against liver

I/R injury than male mice by some sex-dependent mechanisms[64–67]. These reports indicate that the degree and mechanism of liver I/R injury differ between males and females. PARP inhibition may not be effective enough in protecting against liver I/R injury in female mice, unlike male mice. Further investigation is required using female as well as male mice to understand more accurately the effectiveness of PARP inhibition and the underlying protective mechanism against liver I/R injury.

Conclusions

In the present study, we firstly demonstrated that PARP may play a critical role in I/R-induced liver injury and probably inflammation in mouse. H/R-initiated, PARP-mediated cell death (parthanatos and necroptosis) occurred independently of caspases, and is similarly critical to caspase-mediated cell death (apoptosis) redox-dependently. H/R-activated PARP induced parthanatos and necroptosis from an early to late phase after H/R. Further study is needed to elucidate the role of PARP in I/R-induced liver injury and inflammation. However, our findings will undoubtedly advance the understanding of the pathology of post-ischemic liver injury in liver surgery.

Acknowledgements

This study was supported by a JSPS Grants-in-Aid for Scientific Research (KAKENHI) [Grant No. 19H05564 & 20K20472 (to M.O.) ,15H05659 & 20K08299 (to S.H.)]. This work was also supported in part by The Uehara Memorial Foundation, The Takahashi Industrial and Economic Research Foundation (to M.O.) and The Takeda Science Foundation (to S.H.).

Disclosure

The authors report no proprietary or commercial interest in any product mentioned or concept discussed in this article.

References

1. Gibson BA, Kraus WL. New insights into the molecular and cellular functions of poly(ADP-ribose) and PARPs. *Nat Rev Mol Cell Biol*. 2012;13(7):411-424. doi:10.1038/nrm3376
2. Hottiger MO, Hassa PO, Lüscher B, Schüler H, Koch-Nolte F. Toward a unified nomenclature for mammalian ADP-ribosyltransferases. *Trends Biochem Sci*. 2010;35(4):208-219. doi:10.1016/j.tibs.2009.12.003
3. Leung AKL. Poly(ADP-ribose): An organizer of cellular architecture. *J Cell Biol*. 2014;205(5):613-619. doi:10.1083/jcb.201402114
4. Pazzaglia S, Pioli C. Multifaceted Role of PARP-1 in DNA Repair and Inflammation: Pathological and Therapeutic Implications in Cancer and Non-Cancer Diseases. *Cells*. 2019;9(1):41. doi:10.3390/cells9010041
5. Frank D, Vince JE. Pyroptosis versus necroptosis: similarities, differences, and crosstalk. *Cell Death Differ*. 2019;26(1):99-114. doi:10.1038/s41418-018-0212-6
6. Zhao L, Lin H, Chen S, et al. Hydrogen peroxide induces programmed necrosis in rat nucleus pulposus cells through the RIP1/RIP3-PARP-AIF pathway. *J Orthop Res*. 2018;36(4):1269-1282. doi:10.1002/jor.23751
7. Li Y, Tian X, Liu X, Gong P. Bufalin inhibits human breast cancer tumorigenesis by inducing cell death through the ROS-mediated RIP1/RIP3/PARP-1 pathways.

Carcinogenesis. 2018;39(5):700-707. doi:10.1093/carcin/bgy039

8. Li X, Ling Y, Cao Z, et al. Targeting intestinal epithelial cell–programmed necrosis alleviates tissue injury after intestinal ischemia/reperfusion in rats. *J Surg Res*. 2018;225:108-117. doi:10.1016/j.jss.2018.01.007
9. Galaris D, Barbouti A, Korantzopoulos P. Oxidative Stress in Hepatic Ischemia-Reperfusion Injury: The Role of Antioxidants and Iron Chelating Compounds. *Curr Pharm Des*. 2006;12(23):2875-2890. doi:10.2174/138161206777947614
10. Nakazato PCG, Victorino JP, Fina CF, et al. Liver ischemia and reperfusion injury. Pathophysiology and new horizons in preconditioning and therapy. *Acta Cir Bras*. 2018;33(8):723-735. doi:10.1590/s0102-865020180080000008
11. Shi Y, Qiu X, Dai M, Zhang X, Jin G. Hyperoside Attenuates Hepatic Ischemia-Reperfusion Injury by Suppressing Oxidative Stress and Inhibiting Apoptosis in Rats. *Transplant Proc*. 2019;51(6):2051-2059. doi:10.1016/j.transproceed.2019.04.066
12. Williams TM, Wise AF, Layton DS, Ricardo SD. Phenotype and influx kinetics of leukocytes and inflammatory cytokine production in kidney ischemia/reperfusion injury. *Nephrology*. 2018;23(1):75-85. doi:10.1111/nep.12941
13. Li S, Fujino M, Takahara T, Li XK. Protective role of heme oxygenase-1 in fatty liver ischemia–reperfusion injury. *Med Mol Morphol*. 2019;52(2):61-72. doi:10.1007/s00795-018-0205-z
14. Wang W, Wu L, Li J, et al. Alleviation of hepatic ischemia reperfusion injury by oleanolic acid pretreating via reducing HMGB1 release and inhibiting apoptosis and autophagy. *Mediators Inflamm*. 2019;2019:3240713. doi:10.1155/2019/3240713
15. Karatzas T, Neri AA, Baibaki ME, Dontas IA. Rodent models of hepatic ischemia-reperfusion injury: Time and percentage-related pathophysiological mechanisms. *J Surg Res*. 2014;191(2):399-412. doi:10.1016/j.jss.2014.06.024
16. Montalvo-Jave EE, Escalante-Tattersfield T, Ortega-Salgado JA, Piña E, Geller DA. Factors in the Pathophysiology of the Liver Ischemia-Reperfusion Injury. *J Surg Res*. 2008;147(1):153-159. doi:10.1016/j.jss.2007.06.015
17. Siniscalchi A, Gamberini L, Laici C, et al. Post reperfusion syndrome during liver transplantation: From pathophysiology to therapy and preventive strategies. *World J Gastroenterol*. 2016;22(4):1551-1569. doi:10.3748/wjg.v22.i4.1551
18. Terui K, Enosawa S, Haga S, et al. Stat3 confers resistance against hypoxia/reoxygenation-induced oxidative injury in hepatocytes through

upregulation of Mn-SOD. *J Hepatol*. 2004;41(6):957-965. doi:10.1016/j.jhep.2004.08.019

19. Haga S, Kanno A, Ozawa T, Morita N, Asano M, Ozaki M. Detection of Necroptosis in Ligand-Mediated and Hypoxia-Induced Injury of Hepatocytes Using a Novel Optic Probe-Detecting Receptor-Interacting Protein (RIP)1/RIP3 Binding. *Oncol Res*. 2018;26(3):503-513. doi:10.3727/096504017X15005102445191
20. Haga S, Remington SJ, Morita N, Terui K, Ozaki M. Hepatic ischemia induced immediate oxidative stress after reperfusion and determined the severity of the reperfusion-induced damage. *Antioxidants Redox Signal*. 2009;11(10):2563-2572. doi:10.1089/ars.2009.2681
21. Ozaki M, Haga S, Zhang HQ, Irani K, Suzuki S. Inhibition of hypoxia/reoxygenenation-induced oxidative stress in HGF-stimulated antiapoptotic signaling: Role of PI3-K and Akt kinase upon rac1. *Cell Death Differ*. 2003;10(5). doi:10.1038/sj.cdd.4401172
22. Ozaki M, Deshpande SS, Angkeow P, et al. *Inhibition of the Rac1 GTPase Protects against Nonlethal Ischemia/Reperfusion-Induced Necrosis and Apoptosis in Vivo*. *FASEB J.* 2000;14(2):418-429. doi: 10.1096/fasebj.14.2.418.
23. Thornton C, Leaw B, Mallard C, Nair S, Jinnai M, Hagberg H. Cell death in the developing brain after hypoxia-ischemia. *Front Cell Neurosci*. 2017;11:248. doi:10.3389/fncel.2017.00248
24. Gujral JS, Bucci TJ, Farhood A, Jaeschke H. Mechanism of cell death during warm hepatic ischemia-reperfusion in rats: Apoptosis or necrosis? *Hepatology*. 2001;33(2):397-405. doi:10.1053/jhep.2001.22002
25. Ozaki M, Haga S, Ozawa T. In vivo monitoring of liver damage using caspase-3 probe. *Theranostics*. 2012;2(2):207-214. doi:10.7150/thno.3806
26. Voltan R, Secchiero P, Casciano F, Milani D, Zauli G, Tisato V. Redox signaling and oxidative stress: Cross talk with TNF-related apoptosis inducing ligand activity. *Int J Biochem Cell Biol*. 2016;81(Pt B):364-374. doi:10.1016/j.biocel.2016.09.019
27. Franklin JL. Redox regulation of the intrinsic pathway in neuronal apoptosis. *Antioxidants Redox Signal*. 2011;14(8):1437-1448. doi:10.1089/ars.2010.3596
28. Circu ML, Aw TY. Reactive oxygen species, cellular redox systems, and apoptosis. *Free Radic Biol Med*. 2010;48(6):749-762. doi:10.1016/j.freeradbiomed.2009.12.022
29. Van Opdenbosch N, Lamkanfi M. Caspases in Cell Death, Inflammation, and

Disease. *Immunity*. 2019;50(6):1352-1364. doi:10.1016/j.immuni.2019.05.020
30. Rauf A, Shah M, Yellon DM, Davidson SM. Role of Caspase 1 in Ischemia/Reperfusion Injury of the Myocardium. *J Cardiovasc Pharmacol*. 2019;74(3):194-200. doi:10.1097/FJC.0000000000000694
31. Kordes M, Matuschewski K, Hafalla JCR. Caspase-1 Activation of Interleukin-1ß (IL-1ß) and IL-18 Is Dispensable for Induction of Experimental Cerebral Malaria. *Infect Immun*. 2011;79(9):3633-3641. doi:10.1128/IAI.05459-11
32. Boulares AH, Yakovlev AG, Ivanova V, et al. Role of poly(ADP-ribose) polymerase (PARP) cleavage in apoptosis. Caspase 3-resistant PARP mutant increases rates of apoptosis in transfected cells. *J Biol Chem*. 1999;274(33):22932-22940. doi:10.1074/jbc.274.33.22932
33. Haga S, Terui K, Fukai M, et al. Preventing hypoxia/reoxygenation damage to hepatocytes by p66(shc) ablation: up-regulation of anti-oxidant and anti-apoptotic proteins. *J Hepatol*. 2008;48(3):422-432. doi:10.1016/j.jhep.2007.11.018
34. Haga S, Terui K, Zhang HQ, et al. Stat3 protects against Fas-induced liver injury by redox-dependent and -independent mechanisms. *J Clin Invest*. 2003;112(7):989-998. doi:10.1172/JCI200317970
35. Jaeschke H, Gujral JS, Bajt ML. Apoptosis and necrosis in liver disease. *Liver Int*. 2004;24(2):85-89. doi:10.1111/j.1478-3231.2004.0906.x
36. Konishi T, Lentsch AB. Hepatic Ischemia/Reperfusion: Mechanisms of Tissue Injury, Repair, and Regeneration. *Gene Expr*. 2017;17(4):277-287. doi:10.3727/105221617X15042750874156
37. Ozaki M, Suzuki S, Irani K. Redox factor-1/APE suppresses oxidative stress by inhibiting the rac1 GTPase. *FASEB J*. 2002;16(8):889-890. doi:10.1096/fj.01-0664fje
38. Haga S, Remington SJ, Morita N, Terui K, Ozaki M. Hepatic ischemia induced immediate oxidative stress after reperfusion and determined the severity of the reperfusion-induced damage. *Antioxidants Redox Signal*. 2009;11(10). doi:10.1089/ars.2009.2681
39. Li Y, Yang Y, Zhao Y, et al. Astragaloside IV reduces neuronal apoptosis and parthanatos in ischemic injury by preserving mitochondrial hexokinase-II. *Free Radic Biol Med*. 2019;131:251-263. doi:10.1016/j.freeradbiomed.2018.11.033
40. van Wijk SJL, Hageman GJ. Poly(ADP-ribose) polymerase-1 mediated caspase-independent cell death after ischemia/reperfusion. *Free Radic Biol Med*. 2005;39(1):81-90. doi:10.1016/j.freeradbiomed.2005.03.021

41. Kai J, Yang X, Wang Z, et al. Oroxylin a promotes PGC-1α/Mfn2 signaling to attenuate hepatocyte pyroptosis via blocking mitochondrial ROS in alcoholic liver disease. *Free Radic Biol Med*. 2020;153:89-102. doi:10.1016/j.freeradbiomed.2020.03.031
42. Jaeschke H. Reactive oxygen and mechanisms of inflammatory liver injury: Present concepts. *J Gastroenterol Hepatol*. 2011;26 Suppl 1(SUPPL. 1):173-179. doi:10.1111/j.1440-1746.2010.06592.x
43. Bahirwani R, Reddy KR. Drug-induced liver injury due to cancer chemotherapeutic agents. *Semin Liver Dis*. 2014;34(2):162-171. doi:10.1055/s-0034-1375957
44. Gao W-Y, Li D, Cai D-E, et al. Hepatitis B virus X protein sensitizes HL-7702 cells to oxidative stress-induced apoptosis through modulation of the mitochondrial permeability transition pore. *Oncol Rep*. 2017;37(1):48-56. doi:10.3892/or.2016.5225
45. Pinkoski MJ, Brunner T, Green DR, Lin T. Fas and Fas ligand in gut and liver. *Am J Physiol - Gastrointest Liver Physiol*. 2000;278(3 41-3). doi:10.1152/ajpgi.2000.278.3.g354
46. Wang K. Molecular mechanisms of liver injury: apoptosis or necrosis. *Exp Toxicol Pathol*. 2014;66(8):351-356. doi:10.1016/j.etp.2014.04.004
47. Galle PR, Hofmann WJ, Walczak H, et al. Involvement of the CD95 (APO-1/fas) receptor and ligand in liver damage. *J Exp Med*. 1995;182(5):1223-1230. doi:10.1084/jem.182.5.1223
48. Del Re DP, Amgalan D, Linkermann A, Liu Q, Kitsis RN. Fundamental mechanisms of regulated cell death and implications for heart disease. *Physiol Rev*. 2019;99(4):1765-1817. doi:10.1152/physrev.00022.2018
49. Black JH, Casey PJ, Albadawi H, Cambria RP, Watkins MT. Poly Adenosine Diphosphate-Ribose Polymerase Inhibitor PJ34 Abolishes Systemic Proinflammatory Responses to Thoracic Aortic Ischemia and Reperfusion. *J Am Coll Surg*. 2006;203(1):44-53. doi:10.1016/j.jamcollsurg.2006.04.004
50. Hatachi G, Tsuchiya T, Miyazaki T, et al. The poly(adenosine diphosphate-ribose) polymerase inhibitor PJ34 reduces pulmonary ischemia-reperfusion injury in rats. *Transplantation*. 2014;98(6):618-624. doi:10.1097/TP.0000000000000305
51. Mota-Filipe H, Sepodes B, McDonald M, Cuzzocrea S, Pinto R, Thiemermann C. The novel PARP inhibitor 5-aminoisoquinolinone reduces the liver injury caused by ischemia and reperfusion in the rat. Medical Science Monitor. *Med Sci Monit.*

2002;8(11):BR444-453.
52. Crawford RS, Albadawi H, Atkins MD, et al. Postischemic poly (ADP-ribose) polymerase (PARP) inhibition reduces ischemia reperfusion injury in a hind-limb ischemia model. *Surgery*. 2010;148(1):110-118. doi:10.1016/j.surg.2009.12.006
53. David KK, Andrabi SA, Dawson TM, Dawson VL. Parthanatos, A messenger of death. *Front Biosci*. 2009;14(3):1116-1128. doi:10.2741/3297
54. Virág L, Robaszkiewicz A, Rodriguez-Vargas JM, Oliver FJ. Poly(ADP-ribose) signaling in cell death. *Mol Aspects Med*. 2013;34(6):1153-1167. doi:10.1016/j.mam.2013.01.007
55. Zhao H, Ning J, Lemaire A, et al. Necroptosis and parthanatos are involved in remote lung injury after receiving ischemic renal allografts in rats. *Kidney Int*. 2015;87(4):738-748. doi:10.1038/ki.2014.388
56. Vandenabeele P, Galluzzi L, Vanden Berghe T, Kroemer G. Molecular mechanisms of necroptosis: an ordered cellular explosion. *Nat Rev Mol Cell Biol*. 2010;11(10):700-714. doi:10.1038/nrm2970
57. Skaper SD. Poly(ADP-ribose) polymerase-1 in acute neuronal death and inflammation: A strategy for neuroprotection. *Ann N Y Acad Sci*. 2003;993(1):217-228. doi:10.1111/j.1749-6632.2003.tb07532.x
58. Mukhopadhyay P, Horváth B, Rajesh M, et al. PARP inhibition protects against alcoholic and non-alcoholic steatohepatitis. *J Hepatol*. 2017;66(3):589-600. doi:10.1016/j.jhep.2016.10.023
59. Dharwal V, Naura AS. PARP-1 inhibition ameliorates elastase induced lung inflammation and emphysema in mice. *Biochem Pharmacol*. 2018;150:24-34. doi:10.1016/j.bcp.2018.01.027
60. Kay J, Thadhani E, Samson L, Engelward B. Inflammation-induced DNA damage, mutations and cancer. *DNA Repair (Amst)*. 2019;83. doi:10.1016/j.dnarep.2019.102673
61. Eliasson MJL, Sampei K, Mandir AS, et al. Poly(ADP-ribose) polymerase gene disruption renders mice resistant to cerebral ischemia. *Nat Med*. 1997;3(10):1089-1095. doi:10.1038/nm1097-1089
62. Pacher P, Szabo C. Role of the peroxynitrite-poly(ADP-ribose) polymerase pathway in human disease. *Am J Pathol*. 2008;173(1):2-13. doi:10.2353/ajpath.2008.080019
63. Martire S, Mosca L, d'Erme M. PARP-1 involvement in neurodegeneration: A focus on Alzheimer's and Parkinson's diseases. *Mech Ageing Dev*. 2015;146-148:53-64. doi:10.1016/j.mad.2015.04.001

64. Harada H, Pavlick KP, Hines IN, et al. Selected contribution: Effects of gender on reduced-size liver ischemia and reperfusion injury. *J Appl Physiol*. 2001;91(6):2816-2822. doi:10.1152/JAPPL.2001.91.6.2816
65. Crockett ET, Spielman W, Dowlatshahi S, He J. Sex differences in inflammatory cytokine production in hepatic ischemia-reperfusion. *J Inflamm 2006 31*. 2006;3(1):1-14. doi:10.1186/1476-9255-3-16
66. Vilatoba M, Eckstein C, Bilbao G, Frennete L, Eckhoff DE, Contreras JL. 17β-estradiol differentially activates mitogen-activated protein-kinases and improves survival following reperfusion injury of reduced-size liver in mice. *Transplant Proc*. 2005;37(1):399-403. doi:10.1016/J.TRANSPROCEED.2004.12.053
67. Hu Z, Jepps TA, Zhou L, Liu J, Li M, Abbott GW. Kcne4 deletion sex dependently inhibits the RISK pathway response and exacerbates hepatic ischemia-reperfusion injury in mice. *Am J Physiol Regul Integr Comp Physiol*. 2019;316(5):R552-R562. doi:10.1152/AJPREGU.00251.2018

Figure Legends

Fig. 1 - PARP was more crucial in hypoxia/reoxygenation-induced cell death than caspases in AML12 mouse liver cells. (A) Left panel: PJ34 (10 μM) and z-VAD-fmk (20 μM), a pan-caspase inhibitor significantly suppressed H/R-induced cell death (LDH release). Right panel: The % inhibition of cell death was calculated against the cell death of normoxic cells without inhibitor at each group/time point. PJ34 suppressed H/R-induced cell death more than z-VAD-fmk in the concentrations examined. **(B)** Western blot analyses showed apoptosis- and PARP-associated protein expression. Quantitative analysis of western blot is shown in **Supplementary data for Fig. 1**. **(C)** PJ34 did not suppress H/R-induced caspase 3 activation, though z-VAD-fmk did. Each experiment was performed in triplicate and densitometric data were statistically analyzed. Quantitative analysis of western blot data was by ImageJ software. Data, normally distributed, were analyzed by a Tukey-Kramer test and expressed as mean ± S.D. A value of $p < 0.05$ was considered statistically significant [*$p < 0.05$; †$p < 0.01$; n.s., not significant].

Fig. 2 - PARP inhibition did not affect caspase-mediated cell death. (A) Staurosporine (STS, 1 μM) immediately activated caspase3, induced cell death, and cleaved PARP. **(B)** Jo2 (4 μg/mg) slowly activated caspase3, induced cell death, and cleaved PARP. STS-

/Jo2-activated caspase 3 potently cleaved PARP and reduced the production of PAR (right panels). However, PJ34 did not affect STS-/Jo2-induced cell death at all [**(A)(B)** left panels]. For the viable cell assay (xCELLigence assay), each experiment was performed in triplicate and expressed as arbitrary values. Data, normally distributed, were analyzed by a Tukey-Kramer test and expressed as mean ± S.D. n.s., not significant.

Fig. 3 - Hypoxia/reoxygenation-induced PARP activation (the production of PAR) depended on oxidative stress. (A) H/R induced the immediate production of PAR and cleavage of PARP (left). PJ34 dramatically reduced the production of PAR without affecting the cleavage of PARP (middle). z-VAD-fmk did not affect the production of PAR though it clearly inhibited PARP cleavage (right). Quantitative analysis of the protein expressions is shown in **Supplementary data for Fig. 3**. **(B)** Trolox (500 μM), an antioxidant, significantly suppressed H/R-induced production of PAR, but did not affect the cleavage of PARP (arrowheads). **(C)**. Trolox did not suppress H/R-induced caspase 3 cleavage/activation (arrowheads). Each experiment was performed in triplicate by capillary electrophoresis (Wes™). Quantitative analysis of protein expression was performed Compass for Simple Western software. A value of $p < 0.05$ was considered statistically significant (*$p < 0.05$, †$p < 0.01$, n.s., not significant [B and C]). Data, normally distributed, were analyzed by a Tukey-Kramer test and expressed as mean ±

S.D.

Fig. 4 - Oxidative stress directly and immediately induced PARP activation (the production of PAR) and cell death. (A) H_2O_2 (1 mM) immediately induced the production of PAR, then cleaved caspases (Casp) and PARP. Each blot represents three independent experiments. Quantitative analysis of western blot is shown in **Supplementary data for Fig. 4**. **(B)** H_2O_2 immediately induced cell death in AML12 mouse liver cells (xCELLigence assay). PJ34 (10 μM) suppressed H_2O_2-induced cell death at almost all timepoints after H_2O_2-treatment. For each treatment group, the experiment was performed in triplicate. **(C)** PJ34 suppressed both H_2O_2-induced production of PAR and cleavage of PARP. Each experiment was performed in triplicate using a capillary electrophoresis system (Wes™) and representative data are shown. Data, normally distributed, were analyzed by a Tukey-Kramer test and expressed as mean ± S.D. (B). Data, non-normally distributed, were analyzed by a Kruskal-Wallis test with a Dann-Bonferroni post hoc test and expressed as median and interquartile range (C). A value of $p < 0.05$ was considered statistically significant [*$p < 0.01$, †$p < 0.05$, n.s., not significant].

Fig. 5 - Hypoxia/reoxygenation and oxidative stress induces parthanatos and necroptosis through PARP activation. (A) H_2O_2 (1 mM), but not Jo2 (4 μg/mL) and staurosporine (STS; 1 μM), caused the translocation of AIF (green) to nuclei (blue) in AML12 mouse liver cells. PJ34 (10 μM) clearly suppressed H_2O_2-induced nuclear translocation of AIF. Arrowheads indicate translocated AIF in nuclei. **(B)** H/R induced the nuclear translocation of AIF in AML12 cells, which was suppressed by pre-treatment with PJ34 or Trolox. Arrowheads indicate translocated AIF in nuclei. **(C)** H_2O_2 induced RIP1-RIP3 interaction, which was markedly inhibited by PJ34. **(D)** RIP1-RIP3 interaction induced by H/R was effectively inhibited by PJ34 especially at later timepoints. **(E)** RIP1-RIP3 interaction induced by H/R was significantly inhibited by Trolox in a dose-dependent manner. For each treatment group (**C, D, E**), the experiment was performed in triplicate and the data are expressed relative to values prior to treatment. Data, normally distributed, were analyzed by a Tukey-Kramer test and expressed as mean ± S.D. (A, C, D). Data, non-normally distributed, were analyzed by a Kruskal-Wallis test with a Dann-Bonferroni post hoc test and expressed as median and interquartile range (B, E). A value of $p < 0.05$ was considered statistically significant [*$p < 0.01$, †$p < 0.05$, n.s., not significant].

Fig. 6 - Inhibition of PARP dramatically reduced ischemia/reperfusion-induced

injury of liver and inflammatory reaction. (A) The experimental procedure and drug administration of liver I/R experiment are illustrated as a diagram. **(B)** PJ34 (5 mg/kg BW), z-VAD-fmk (5 mg/kg BW), or Trolox (50 mg/kg BW) were intraperitoneally administered twice to mice 5 min before and within 1 min after liver ischemia. PJ34 significantly suppressed the increase of serum levels of ALT, AST & LDH 24 h after liver I/R, similar to z-VAD-fmk and Trolox (n=7 at each group). Different letters (a, b, c) in the graph indicate statistically significant differences among groups ($p < 0.05$). **(C)** Photomicrographs of post-ischemic liver tissue are shown (H & E stain) with/without PJ34. The areas surrounded by dashed lines in the upper panels are magnified and shown in the lower panels. The arrowheads indicate necrotic areas. **(D)** PJ34 suppressed hepatic PARP expression and the production of PAR after I/R. Each blot is representative of five independent experiments. Quantitative analysis of protein expression was performed by capillary electrophoresis (Wes™) and Compass for ProteinSimple software. *$p < 0.05$; n.s., not significant. Data, non-normally distributed, were analyzed by a Kruskal-Wallis test with a Dann-Bonferroni post hoc test and expressed as median and interquartile range (B). Data, normally distributed, were analyzed by a Tukey-Kramer test and expressed as mean ± S.D. (D). A value of $p < 0.05$ was considered statistically significant.

Fig. 7 - Schematic illustration of redox-dependent, PARP-mediated

ischemia/reperfusion-induced injury and inflammation. Hepatic I/R activates caspases within a few hours after reperfusion, which will eventually cause apoptotic cell death with DNA fragmentation. The DNA damage by ischemia or I/R-induced cellular ROS initially activates PARP to repair the damaged DNA, which is cleaved/inactivated partially by the activated caspases. The caspase-mediated inactivation of PARP may contribute to the achievement of apoptotic cell death. In comparison, the DNA damage caused by ischemia or I/R-induced ROS will overactivate PARP and consume NAD(+) and ATP, which directly leads to necrosis. In parallel, the activated PARP may cause signal-regulated cell death such as parthanatos and necroptosis through AIF translocation and RIP1-RIP3 interaction, respectively. Parthanatos and necroptosis may be involved in early and late phases of I/R-induced injury, respectively. These lytic types of cell death may provoke sterile inflammation and enhance injury in the post-ischemic liver.

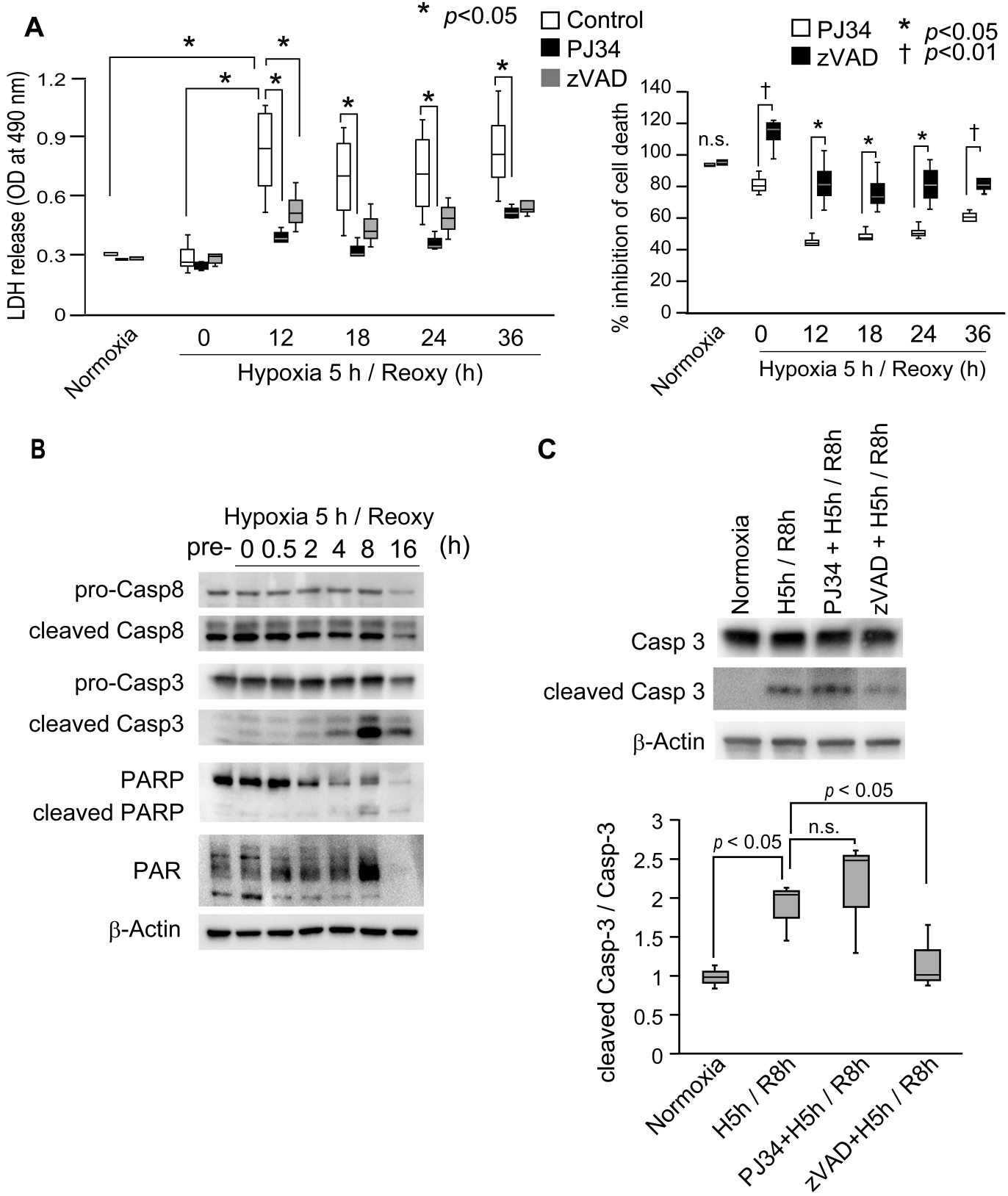
A
* p<0.05
Control
PJ34
zVAD
LDH release (OD at 490 nm)
1.2
0.9
0.6
0.3
0
Normoxia
0
12
18
24
36
Hypoxia 5 h / Reoxy (h)
PJ34
zVAD
* p<0.05
† p<0.01
% inhibition of cell death
140
120
100
80
60
40
20
0
n.s.
B
Hypoxia 5 h / Reoxy
pre- 0 0.5 2 4 8 16 (h)
pro-Casp8
cleaved Casp8
pro-Casp3
cleaved Casp3
PARP
cleaved PARP
PAR
β-Actin
C
Normoxia
H5h / R8h
PJ34 + H5h / R8h
zVAD + H5h / R8h
Casp 3
cleaved Casp 3
β-Actin
p < 0.05
n.s.
p < 0.05
cleaved Casp-3 / Casp-3
3
2.5
2
1.5
1
0.5
0
Normoxia
H5h / R8h
PJ34+H5h / R8h
zVAD+H5h / R8h

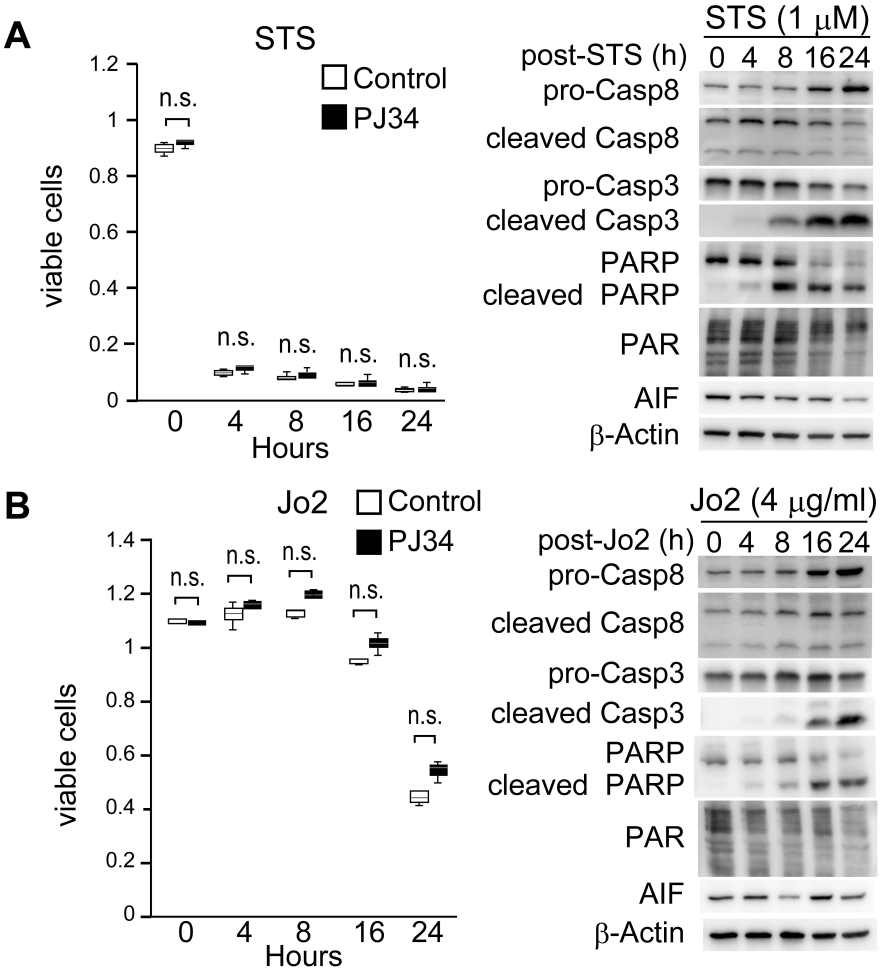
A
STS
Control
PJ34
viable cells
1.2
1
0.8
0.6
0.4
0.2
0
n.s.
n.s.
n.s.
n.s.
n.s.
0
4
8
16
24
Hours
STS (1 μM)
post-STS (h)
0 4 8 16 24
pro-Casp8
cleaved Casp8
pro-Casp3
cleaved Casp3
PARP
cleaved PARP
PAR
AIF
β-Actin
B
Jo2
Control
PJ34
viable cells
1.4
1.2
1
0.8
0.6
0.4
0.2
0
n.s.
n.s.
n.s.
n.s.
n.s.
0
4
8
16
24
Hours
Jo2 (4 μg/ml)
post-Jo2 (h)
0 4 8 16 24
pro-Casp8
cleaved Casp8
pro-Casp3
cleaved Casp3
PARP
cleaved PARP
PAR
AIF
β-Actin

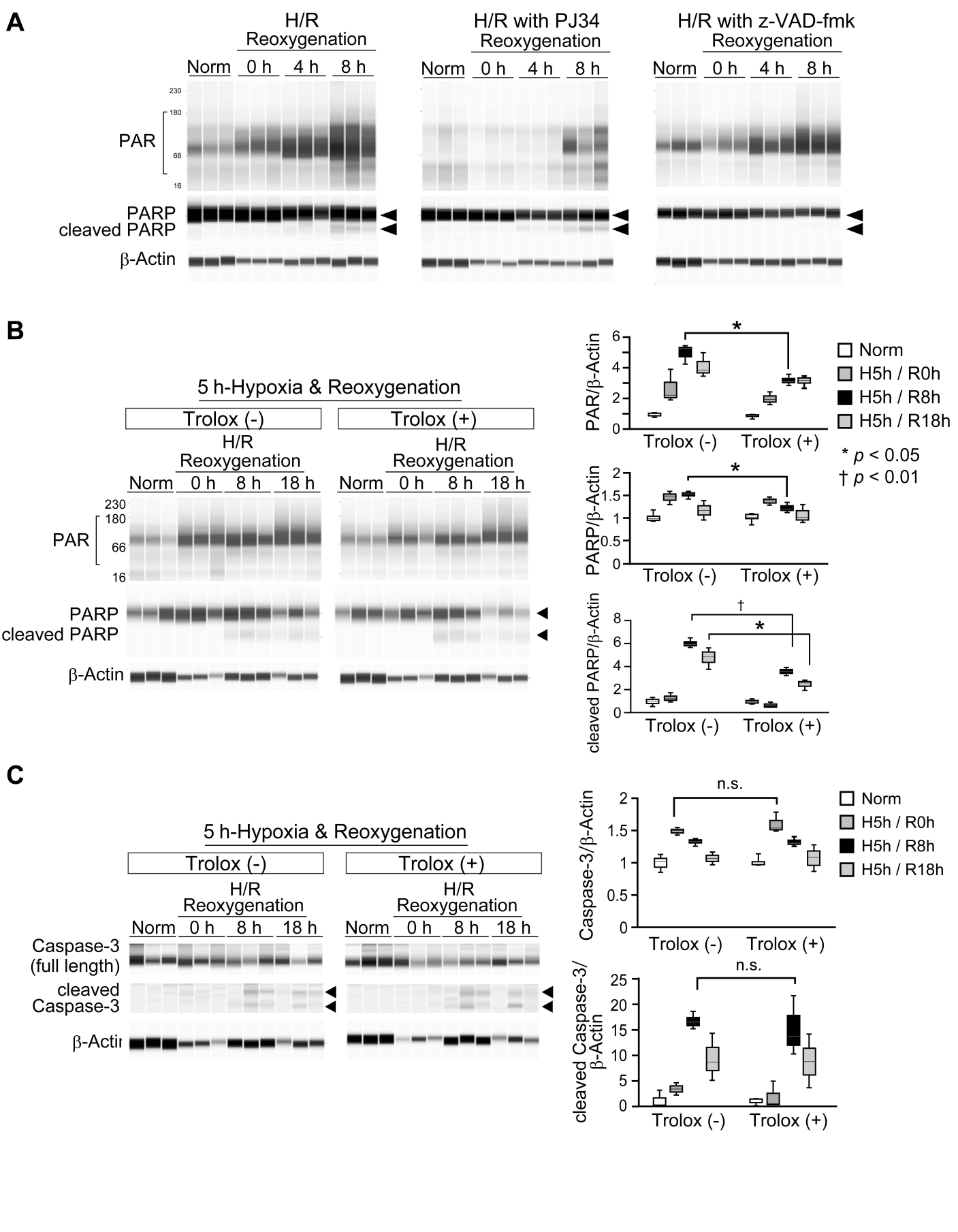
A
H/R
Reoxygenation
Norm
0 h
4 h
8 h
H/R with PJ34
Reoxygenation
H/R with z-VAD-fmk
Reoxygenation
230
180
66
16
PAR
PARP
cleaved PARP
β-Actin
B
5 h-Hypoxia & Reoxygenation
Trolox (-)
Trolox (+)
18 h
PAR/β-Actin
PARP/β-Actin
cleaved PARP/β-Actin
Norm
H5h / R0h
H5h / R8h
H5h / R18h
* p < 0.05
† p < 0.01
C
Caspase-3
(full length)
cleaved
Caspase-3
β-Actin
Caspase-3/β-Actin
cleaved Caspase-3/
β-Actin
n.s.

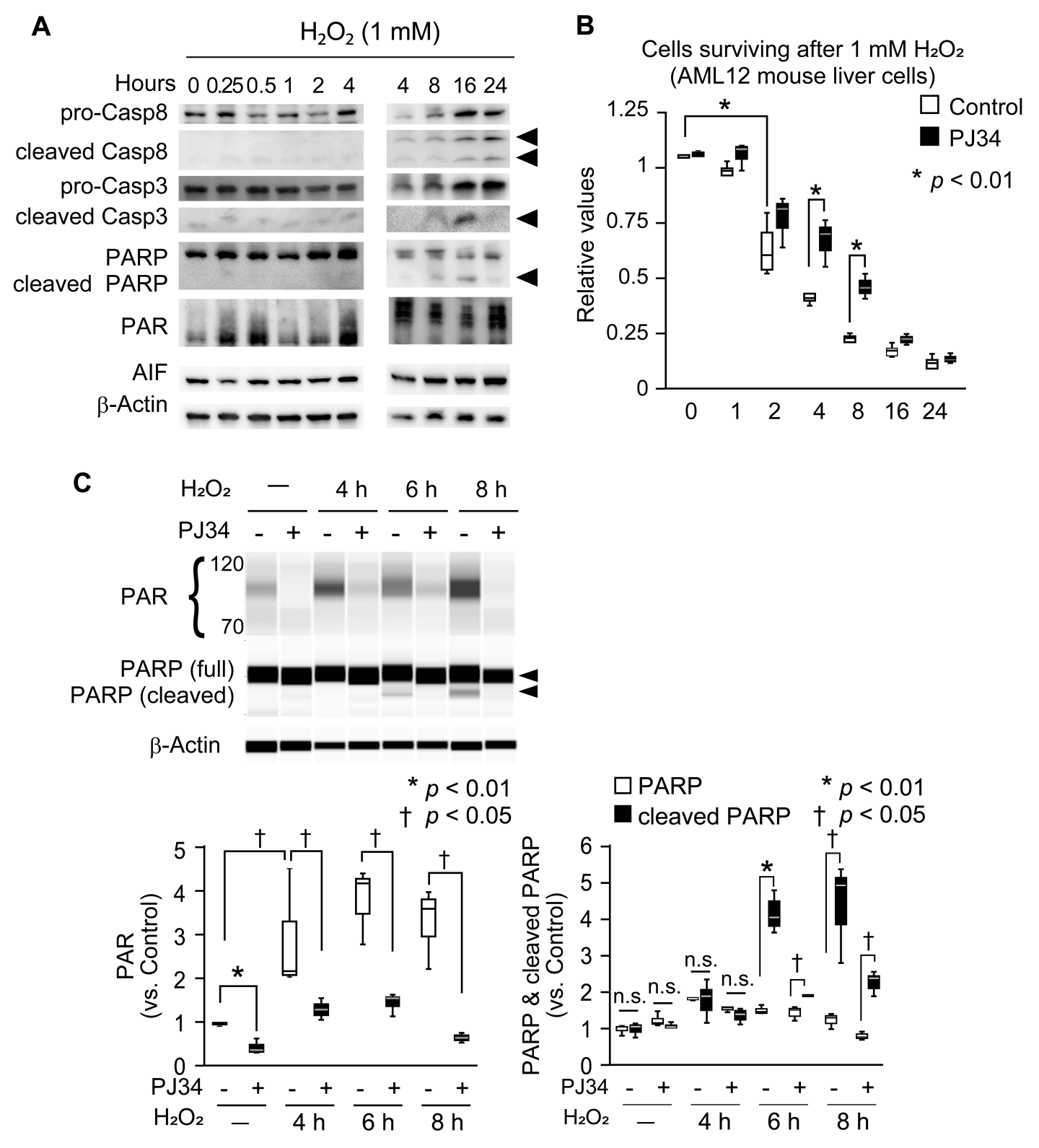
A
H2O2 (1 mM)
Hours 0 0.25 0.5 1 2 4 4 8 16 24
pro-Casp8
cleaved Casp8
pro-Casp3
cleaved Casp3
PARP
cleaved PARP
PAR
AIF
β-Actin
B
Cells surviving after 1 mM H2O2
(AML12 mouse liver cells)
Control
PJ34
* p < 0.01
Relative values
1.25
1
0.75
0.5
0.25
0
0 1 2 4 8 16 24
C
H2O2 — 4 h 6 h 8 h
PJ34 - + - + - + - +
120
70
PAR
PARP (full)
PARP (cleaved)
β-Actin
* p < 0.01
† p < 0.05
PAR (vs. Control)
PJ34 - + - + - + - +
H2O2 — 4 h 6 h 8 h
PARP
cleaved PARP
* p < 0.01
† p < 0.05
PARP & cleaved PARP (vs. Control)
n.s.
PJ34 - + - + - + - +
H2O2 — 4 h 6 h 8 h

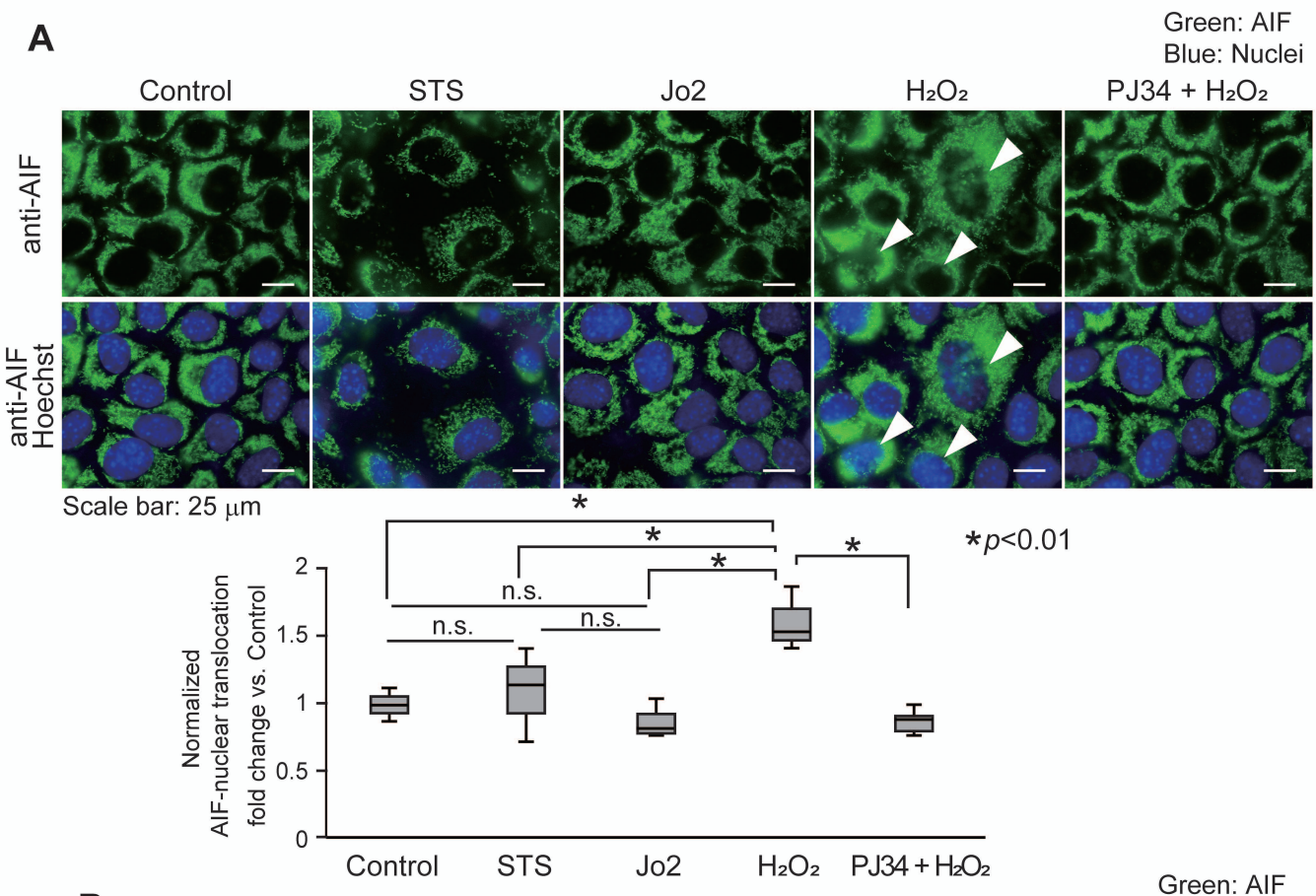
A
Green: AIF
Blue: Nuclei
Control
STS
Jo2
H2O2
PJ34 + H2O2
anti-AIF
anti-AIF Hoechst
Scale bar: 25 μm
*
*
*
*
*
*p<0.01
n.s.
n.s.
n.s.
Normalized AIF-nuclear translocation fold change vs. Control
2
1.5
1
0.5
0
Control
STS
Jo2
H2O2
PJ34 + H2O2

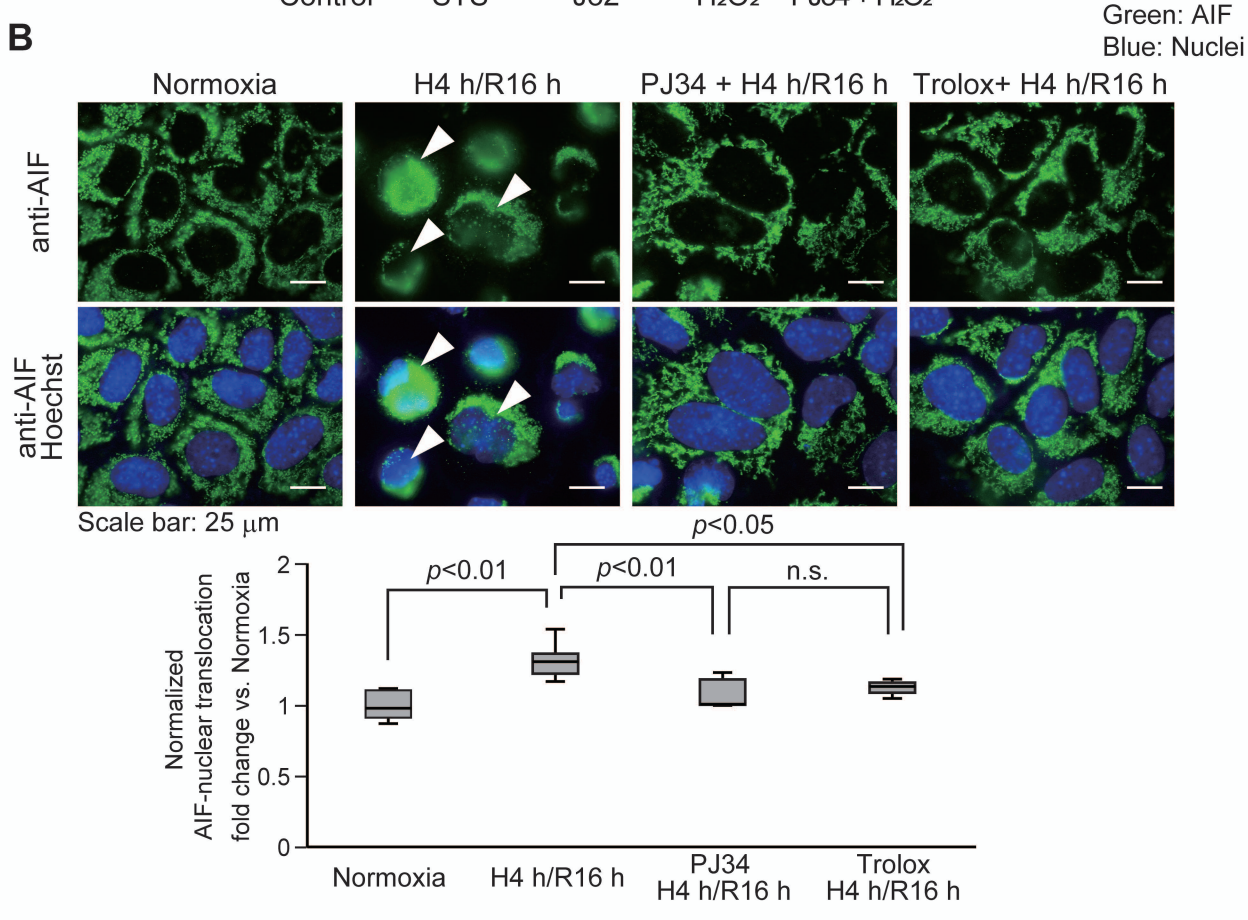
B
Green: AIF
Blue: Nuclei
Normoxia
H4 h/R16 h
PJ34 + H4 h/R16 h
Trolox+ H4 h/R16 h
anti-AIF
anti-AIF Hoechst
Scale bar: 25 μm
p<0.05
p<0.01
p<0.01
n.s.
Normalized AIF-nuclear translocation fold change vs. Normoxia
2
1.5
1
0.5
0
Normoxia
H4 h/R16 h
PJ34 H4 h/R16 h
Trolox H4 h/R16 h

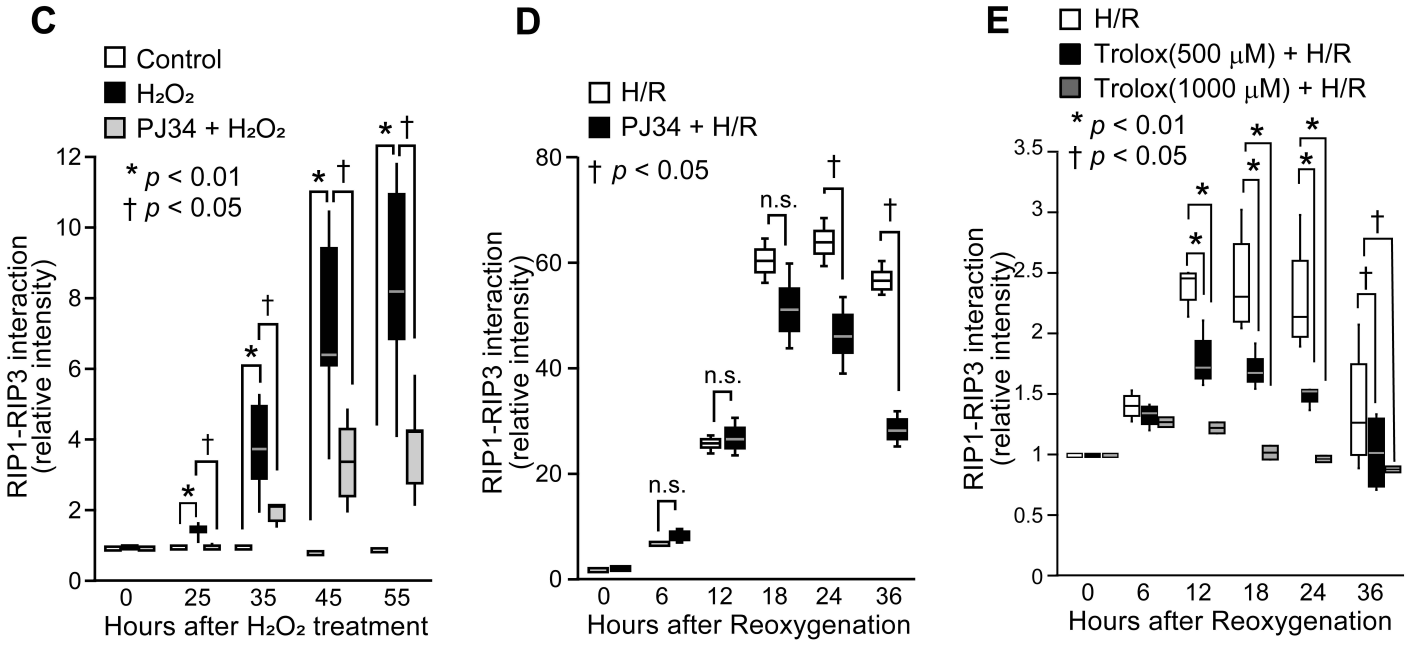
C
Control
H₂O₂
PJ34 + H₂O₂
* p < 0.01
† p < 0.05
RIP1-RIP3 interaction (relative intensity)
Hours after H₂O₂ treatment
D
H/R
PJ34 + H/R
† p < 0.05
n.s.
RIP1-RIP3 interaction (relative intensity)
Hours after Reoxygenation
E
H/R
Trolox(500 μM) + H/R
Trolox(1000 μM) + H/R
* p < 0.01
† p < 0.05
RIP1-RIP3 interaction (relative intensity)
Hours after Reoxygenation

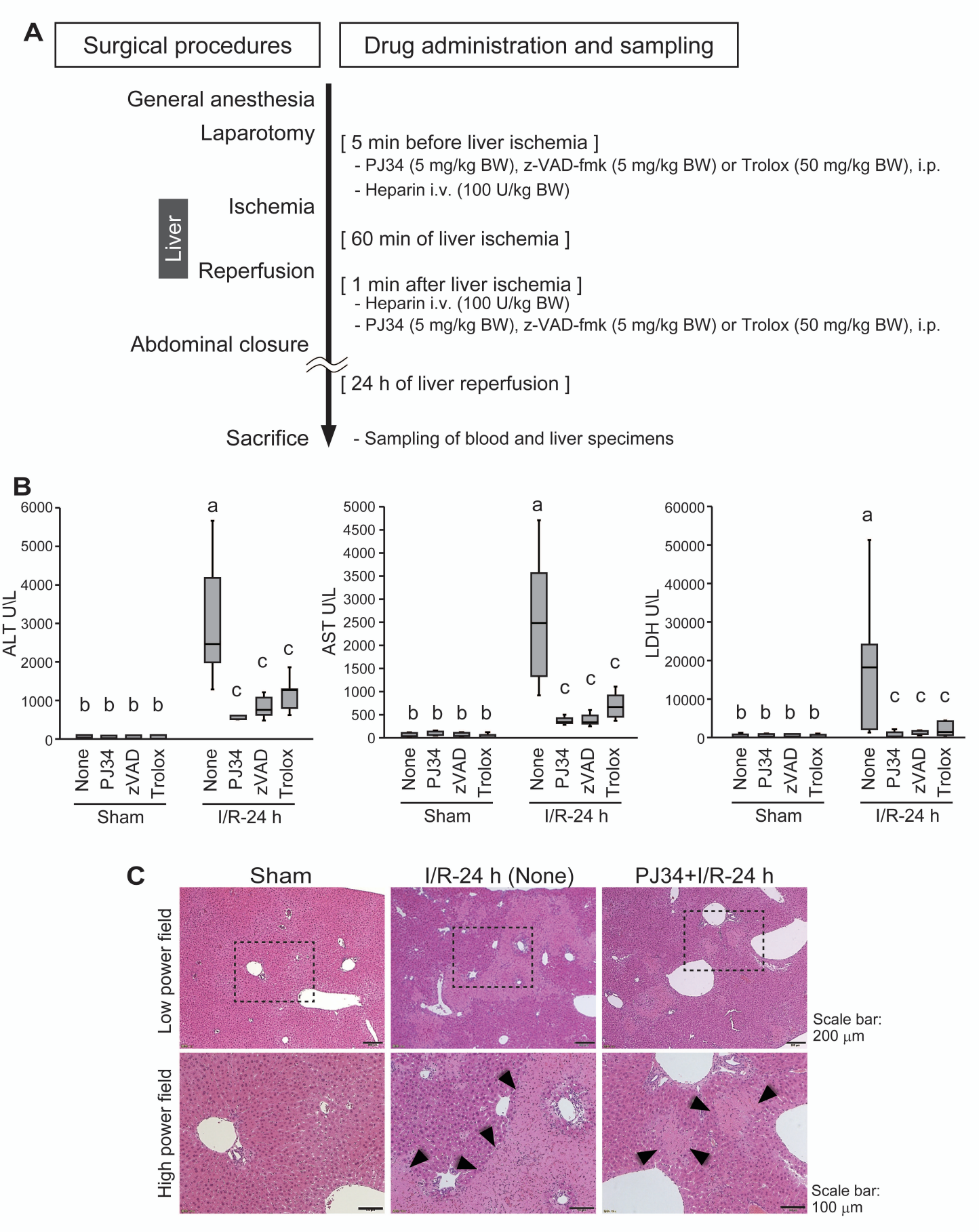
A
Surgical procedures
Drug administration and sampling
General anesthesia
Laparotomy
Liver
Ischemia
Reperfusion
Abdominal closure
Sacrifice
[5 min before liver ischemia]
- PJ34 (5 mg/kg BW), z-VAD-fmk (5 mg/kg BW) or Trolox (50 mg/kg BW), i.p.
- Heparin i.v. (100 U/kg BW)
[60 min of liver ischemia]
[1 min after liver ischemia]
- Heparin i.v. (100 U/kg BW)
- PJ34 (5 mg/kg BW), z-VAD-fmk (5 mg/kg BW) or Trolox (50 mg/kg BW), i.p.
[24 h of liver reperfusion]
- Sampling of blood and liver specimens
B
ALT U\L
AST U\L
LDH U\L
None
PJ34
zVAD
Trolox
Sham
I/R-24 h
C
Sham
I/R-24 h (None)
PJ34+I/R-24 h
Low power field
High power field
Scale bar: 200 μm
Scale bar: 100 μm

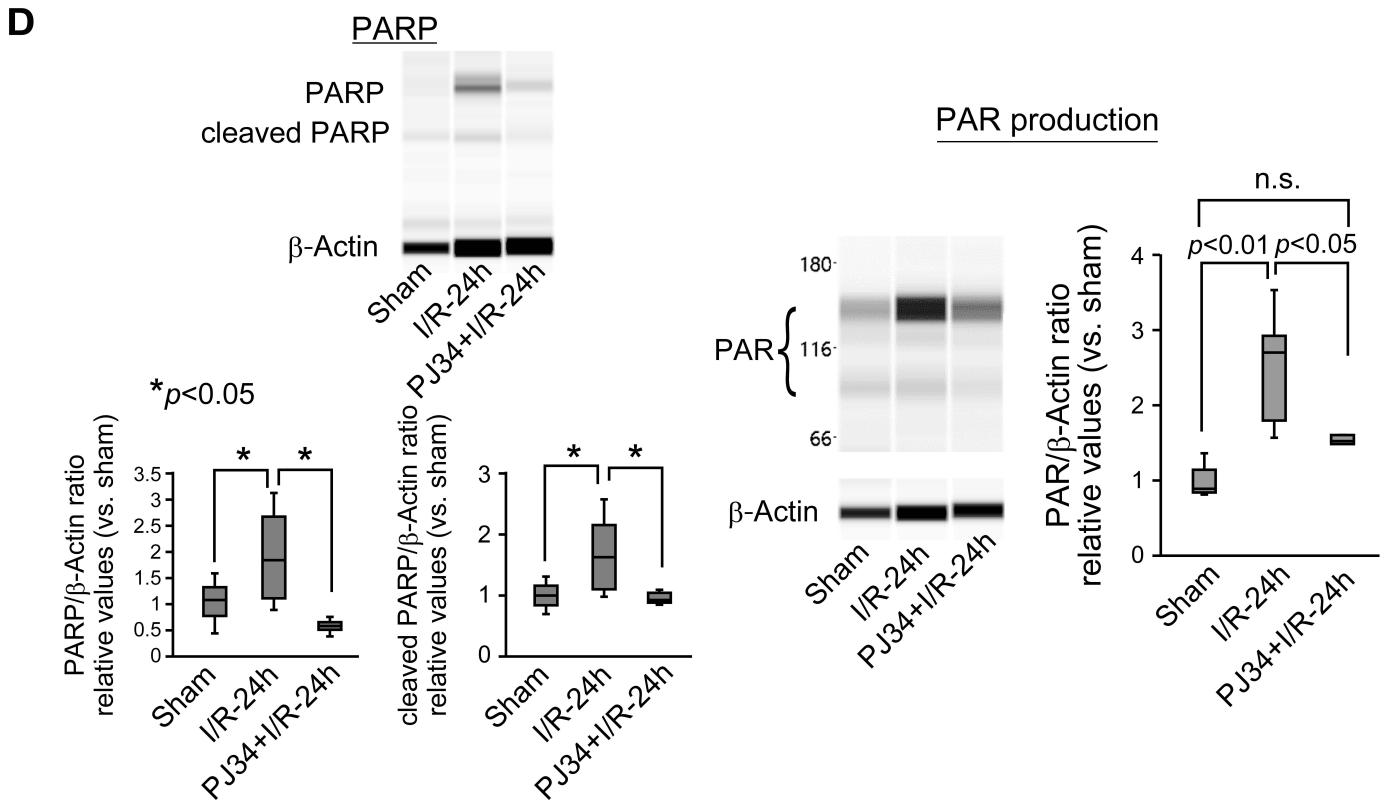
D
PARP
PARP
cleaved PARP
β-Actin
Sham
I/R-24h
PJ34+I/R-24h
*p<0.05
PARP/β-Actin ratio
relative values (vs. sham)
cleaved PARP/β-Actin ratio
relative values (vs. sham)
PAR production
180
116
66
PAR
β-Actin
n.s.
p<0.01
p<0.05
PAR/β-Actin ratio
relative values (vs. sham)

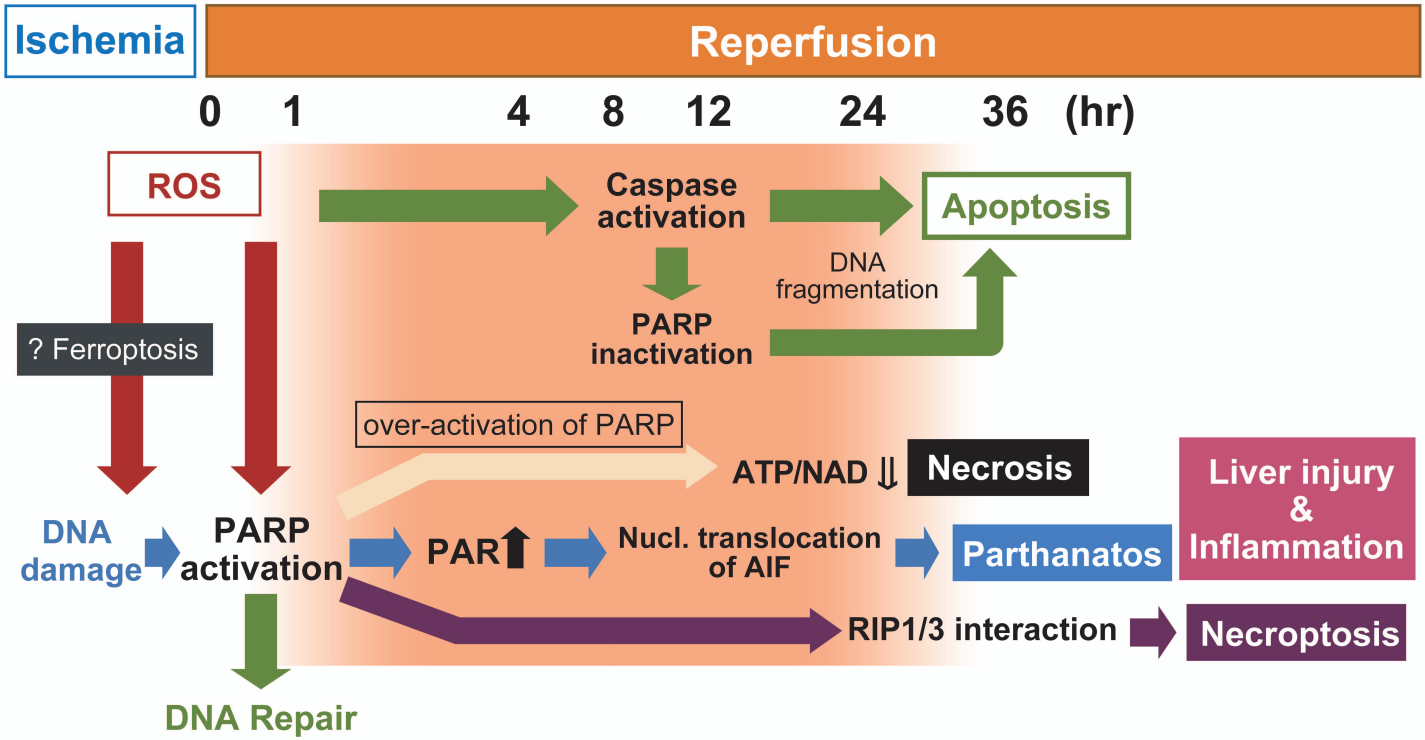

AIF: apoptosis-inducing factor; ATP: adenosine triphosphate; NAD: nicotinamide adenine dinucleotide; PARP: poly(ADP-ribose) polymerase; RIP: receptor-interacting serine/threonine-protein kinase; ROS: reactive oxygen species